

ROBUST ADAPTIVE DETECTION AGAINST SIRV CLUTTER IN THE PRESENCE OF STEERING VECTOR MISMATCHES

X. Dai^{1,*}, G. Cui², and L. Kong²

¹College of Automation, Chongqing University, Chongqing, China

²School of Electronic Engineering, University of Electronic Science and Technology of China, Chengdu, China

Abstract—This paper mainly deals with the problem of detecting a target against spherically invariant random vector (SIRV) clutter in the presence of steering vector mismatches. Assuming that the mismatch of the steering vector satisfies the conic constraint, the generalized likelihood ratio test (GLRT) is devised, and the geometry description is proposed for the derived solution. Additionally, the fully adaptive GLRT is derived by replacing the exact covariance with fixed point estimate (FPE). Finally, several numerical results are provided and discussed.

1. INTRODUCTION

The design of adaptive detection algorithms has been an active field of research, and many detectors have been proposed. Since the uniformly most powerful (UMP) test does not exist because of lacking the prior knowledge of clutter and target, as a consequence, a variety of different algorithms have been explored in open literatures. Among them, we mention the famous one-step generalized likelihood ratio test (GLRT) in [1], and two-step adaptive matched filter (AMF) [2], and the adaptive normalized matched filter (ANMF) [3], also known as adaptive cosine coherence (ACE) [4].

The above detection algorithms are based on the exact knowledge of the signal array steering vector. However, in practical applications, the detection performance may suffer severe degradation because of

Received 27 November 2011, Accepted 26 December 2011, Scheduled 9 January 2012

* Corresponding author: Xin Dai (toybear@vip.sina.com).

the actual steering vector not perfectly aligned with the nominal one. Recently, many works are concerned on the adaptive detection problem with steering vector mismatches against Gaussian clutter. In [5], the adaptive robust detection was devised in Gaussian clutter with unknown covariance matrix in the presence of steering vector mismatches, and the work was extended by considering the interference in [6]. In [7], the distributed target was investigated in the presence of mismatches, and in [8], the test was designed in partially homogeneous environment. The above results show that the acceptance/rejection performance is improved greatly by considering the steering vector mismatches at the design stage.

However, in practical applications, the detection environment, such as sea clutter, is not well modeled as Gaussian process, and they are more consistent to some high tails non-Gaussian distributions. The spherically invariant random vector (SIRV) model has been proved to describe the real radar measurements well, especially in high resolution radars or at low grazing angles, which is a family of lots of non-Gaussian processes, such as Weibull and K-distributions. It can be described as the product of a temporally and spatially slowly varying texture component, times a more rapidly varying process, the so-called speckle, Gaussian distributed due to the local validity of Central Limit Theorem [9–14].

Motivated by extending the target detection problem with steering vector mismatches in Gaussian background to that against SIRV clutter, we consider a general binary hypotheses target detection model as in [5], the difference is that the test is devised in SIRV clutter. Since the optimum Neyman-Pearson receiver is not available, the suboptimum GLRT-based receiver is devised by assuming that the actual steering vector is constraint within a cone.

To make the derived GLRT-based receiver fully adaptive, we resort to the secondary data, which is free of signals, sharing the same covariance matrix with the primary data, to estimate the exact covariance matrix. The fixed-point estimate (FPE) is adopted [15–17], since in SIRVs, it is unbiased, consistent and ensures the CFAR property with respect to both the structure of the covariance matrix and the clutter power levels.

The rest of the paper is organized as follows. In Section 2, we present the detection problem and devise the GLRT detector; and in Section 3, we devise the full adaptive GLRT. Several numerical results are given and discussed in Section 4. Finally, some conclusions are provided in Section 5.

2. PROBLEM FORMULATION AND DETECTOR DESIGN

We assume that the radar returns are collected from N sensors, and the problem of detecting a target can be formulated in terms of the following binary hypotheses test:

$$\begin{cases} H_0 : \mathbf{z} = \mathbf{c} \\ H_1 : \mathbf{z} = \mathbf{u} + \mathbf{c} \end{cases} \quad (1)$$

where \mathbf{z} , \mathbf{u} and \mathbf{c} are the N -dimensional complex vectors sampled from the sensors, base-band equivalent of the received signals, the transmitted signals and the clutter, respectively.

In general, the clutter vector is modeled as a SIRV [11], which can be written as

$$\mathbf{c} = \tau \mathbf{g} \quad (2)$$

where the texture component τ is a non-negative random variable with probability density function (pdf) $f_\tau(\cdot)$ and unit root mean square value. The speckle component \mathbf{g} is a zero-mean complex Gaussian vector with covariance matrix \mathbf{M} , and statistically independent with texture τ . Thus, the probability density function of \mathbf{c} is given by

$$f(\mathbf{c}) = \frac{1}{\pi^N \det(\mathbf{R})} h_N(\mathbf{c}^\dagger \mathbf{R}^{-1} \mathbf{c}) \quad (3)$$

where $\mathbf{R} = 2\sigma^2 \mathbf{M}$ is the covariance matrix ($2\sigma^2$ denotes the power level), $(\cdot)^\dagger$ is conjugate transpose, $\det(\cdot)$ is the determinant of a square matrix, and $h_N(\cdot)$ is defined as

$$h_N(y) = \int_0^\infty x^{-2N} \exp\left(-\frac{y}{x}\right) f_\tau(x) dx \quad (4)$$

For example, the most common K distribution clutter satisfies the above model, in such case, the $h_N(\cdot)$ is defined as

$$h_N(y) = \frac{b^{2N} (b\sqrt{y})^{\nu-N}}{\Gamma(\nu) 2^{\nu-1}} K_{N-\nu}(b\sqrt{y}) \quad (5)$$

and the characteristic function of τ is

$$f_\tau(x) = \frac{2b(bx)^{2\nu-1}}{\Gamma(\nu) 2^\nu} \exp\left(-\frac{b^2 x^2}{2}\right), \quad x > 0 \quad (6)$$

where b and ν denote respectively the scale and shape parameters, $\Gamma(\cdot)$ is the Eulerian gamma function, and $K_\nu(\cdot)$ is the modified second-kind Bessel function with order ν . To preserve the covariance matrix, it usually sets $E[\tau^2] = 1$, then, $b = \sqrt{2\nu}$, where $E[\cdot]$ denotes the statistics expectation.

Applying whitening and rotating transform on the received signal, the detection problem can be recast as

$$\begin{cases} H_0 : \mathbf{r} = \mathbf{n} \\ H_1 : \mathbf{r} = \mathbf{p} + \mathbf{n} \end{cases} \quad (7)$$

where $\mathbf{r} = \mathbf{U}\mathbf{M}^{-1/2}\mathbf{z}$, $\mathbf{n} = \mathbf{U}\mathbf{M}^{-1/2}\mathbf{c} = \tau\mathbf{U}\mathbf{M}^{-1/2}\mathbf{g}$, and \mathbf{U} is a unitary transformation such that $\mathbf{p} = \mathbf{U}\mathbf{M}^{-1/2}\mathbf{u} = \alpha\mathbf{e}_N$, $\mathbf{e}_N = [0, 0, \dots, 1]^T$ ($(\cdot)^T$ denotes the transpose) in perfect matching case with $\mathbf{u} = \mathbf{s}$, and α is a complex unknown parameter.

In practical applications, due to the pointing errors, imperfect array calibration and distorted antenna shape, spatial multipath, and in-phase and quadrature components errors, the mismatches are usually occurred, and cause deviations of the actual steering vector from the nominal direction \mathbf{e}_N . Moreover, assume that \mathbf{p} belongs to the cone set Γ defined as follows [1].

Definition: Let $\mathbf{x} = [\mathbf{x}_{N-1}^T, x_N]^T$ is a N -dimensional complex vector with last component x_N , and the cone set is

$$\Gamma = \left\{ \mathbf{x} = [\mathbf{x}_{N-1}^T, x_N]^T \in \mathbb{C}^N : \|\mathbf{x}_{N-1}\| \leq \gamma |x_N| \right\} = \left\{ \mathbf{x} \in \mathbb{C}^N : \mathbf{x}^\dagger \boldsymbol{\Sigma} \mathbf{x} \leq 0 \right\} \quad (8)$$

where \mathbb{C}^N is the N -dimensional complex vector space, $\|\cdot\|$ is the Euclidean norm, $|\cdot|$ is the modulus of a complex number, and $\boldsymbol{\Sigma} = \text{diag}(1, \dots, 1, -\gamma^2)$ is an N -dimensional diagonal matrix with $\tan \phi = \gamma$, ϕ is the acute angle of the cone.

In general, the Neyman-Pearson test is not available, thus, the sub-optimal GLRT-based receiver is derived, which is equivalent to replacing the unknown parameters with their maximum likelihood estimates (MLEs). Specifically, the GLRT for the problem (1) can be written as

$$\frac{\max_{\tau, \mathbf{p} \in \Gamma} f(\mathbf{z} | H_1, \tau, \mathbf{p})}{\max_{\tau} f(\mathbf{z} | H_1, \tau)} \underset{H_0}{\overset{H_1}{\gtrless}} G \quad (9)$$

where G is the detection threshold, setting according to the probability of false alarm (P_{fa}), $f(\mathbf{r} | H_1, \tau, \mathbf{p})$ and $f(\mathbf{r} | H_0, \tau)$ are respectively

the pdfs of the complex receive signals under H_1 and H_0 hypotheses. Previous assumptions imply that

$$\begin{aligned}
 f(\mathbf{z} | H_1, \tau, \mathbf{p}) &= \frac{1}{\pi^N \det(\tau^2 \mathbf{M})} \exp \left\{ -\frac{(\mathbf{z} - \mathbf{u})^\dagger \mathbf{M}^{-1} (\mathbf{z} - \mathbf{u})}{\tau^2} \right\} \\
 &= \frac{1}{\pi^N \det(\tau^2 \mathbf{M})} \exp \left\{ -\frac{(\mathbf{r} - \mathbf{p})^\dagger (\mathbf{r} - \mathbf{p})}{\tau^2} \right\} \quad (10)
 \end{aligned}$$

$$\begin{aligned}
 f(\mathbf{z} | H_0, \tau, \mathbf{p}) &= \frac{1}{\pi^N \det(\tau^2 \mathbf{M})} \exp \left\{ -\frac{\mathbf{z}^\dagger \mathbf{M}^{-1} \mathbf{z}}{\tau^2} \right\} \\
 &= \frac{1}{\pi^N \det(\tau^2 \mathbf{M})} \exp \left\{ -\frac{\mathbf{r}^\dagger \mathbf{r}}{\tau^2} \right\} \quad (11)
 \end{aligned}$$

It is not difficult to obtain that under H_0 , the MLE of τ^2 is

$$\hat{\tau}^2 = \frac{\mathbf{r}^\dagger \mathbf{r}}{N} \quad (12)$$

and under H_1 , it is

$$\hat{\tau}^2 = \frac{(\mathbf{r} - \mathbf{p})^\dagger (\mathbf{r} - \mathbf{p})}{N} \quad (13)$$

Substituting the MLEs of the texture component τ under H_0 and H_1 hypotheses into (9), and after some algebraic manipulations, the GLRT-based test (9) can be rewritten as follows.

$$\max_{\mathbf{p} \in \Gamma} \frac{\mathbf{r}^\dagger \mathbf{r}}{(\mathbf{r} - \mathbf{p})^\dagger (\mathbf{r} - \mathbf{p})} = \frac{\mathbf{r}^\dagger \mathbf{r}}{\min_{\mathbf{p} \in \Gamma} (\mathbf{r} - \mathbf{p})^\dagger (\mathbf{r} - \mathbf{p})} \stackrel{H_1}{\geq} \stackrel{H_0}{G} \quad (14)$$

Performed as in [6], we have

$$\min_{\mathbf{p} \in \Gamma} (\mathbf{r} - \mathbf{p})^\dagger (\mathbf{r} - \mathbf{p}) = \frac{1}{1 + \gamma^2} (\|\mathbf{r}_{N-1}\| - \gamma |\mathbf{r}_N|)^2 u(\mathbf{r}^\dagger \mathbf{\Sigma} \mathbf{r}) \quad (15)$$

where $u(\cdot)$ is the unit step function, i.e.,

$$u(x) = \begin{cases} 1, & x \geq 0 \\ 0, & x < 0 \end{cases} \quad (16)$$

The Equation (15) can be explained by the geometry relationship, the constraint cone is shown in Figure 1. If $\mathbf{r}^\dagger \mathbf{\Sigma} \mathbf{r} < 0$, or saying that the vector \mathbf{r} lies within the cone, it is obvious that the minimum value is achieved at $\mathbf{r} = \mathbf{p}$, such that

$$\min_{\mathbf{p} \in \Gamma} (\mathbf{r} - \mathbf{p})^\dagger (\mathbf{r} - \mathbf{p}) = 0 \quad (17)$$

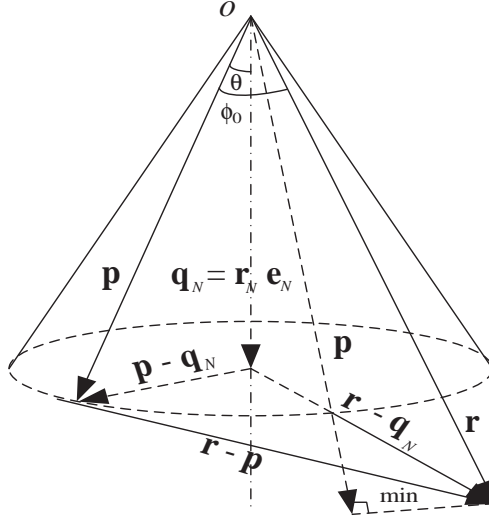


Figure 1. The geometry of the constraint cone.

For $\mathbf{r}^\dagger \Sigma \mathbf{r} \geq 0$, the following norm triangle inequality is satisfied

$$\begin{aligned} \|\mathbf{r} - \mathbf{p}\| &= \|(\mathbf{r} - \mathbf{q}_N) - (\mathbf{p} - \mathbf{q}_N)\| \geq \|\mathbf{r} - \mathbf{q}_N\| - \|\mathbf{p} - \mathbf{q}_N\| \\ &\geq \|\mathbf{r} - \mathbf{q}_N\| - \|\mathbf{p}_c - \mathbf{q}_N\| \end{aligned} \quad (18)$$

where \mathbf{q}_N is the projection of \mathbf{r} onto \mathbf{e}_N , \mathbf{p} is the vector within the cone, and \mathbf{p}_c is the vector on the surface of cone, such that $\mathbf{p}_c^\dagger \Sigma \mathbf{p}_c = 0$. Thus, the possible \mathbf{p}_c lies in the same plane with \mathbf{r} and \mathbf{q}_N , then, the minimum value of $\|\mathbf{r} - \mathbf{p}\|$ is obtained, i.e.,

$$\min_{\mathbf{p}} \|\mathbf{r} - \mathbf{p}\|^2 = (\|\mathbf{r}_{N-1}\| - \gamma \|\mathbf{r}_N\|)^2 \cos^2 \theta_c = \frac{1}{1 + \gamma^2} (\|\mathbf{r}_{N-1}\| - \gamma \|\mathbf{r}_N\|)^2 \quad (19)$$

Considering the condition $\mathbf{r}^\dagger \Sigma \mathbf{r} > 0$, the solution is the same as in (6).

Thus, substituting (19) into (14), and after some algebra, the GLRT can be recast as

$$\frac{\mathbf{r}^\dagger \mathbf{r}}{(\|\mathbf{r}_{N-1}\| - \gamma \|\mathbf{r}_N\|)^2} u(\mathbf{r}^\dagger \Sigma \mathbf{r}) \underset{H_0}{\overset{H_1}{\geq}} G \quad (20)$$

where G is the suitable modification of the original threshold in (14).

Moreover, (20) can be expressed in terms of the raw data vector, i.e.,

$$\frac{\mathbf{z}^\dagger \mathbf{M}^{-1} \mathbf{z}}{\left(\sqrt{\mathbf{z}^\dagger \mathbf{M}^{-1} \mathbf{z} - \frac{|\mathbf{z}^\dagger \mathbf{M}^{-1} \mathbf{s}|^2}{\mathbf{s}^\dagger \mathbf{M}^{-1} \mathbf{s}}} - \gamma \sqrt{\frac{|\mathbf{z}^\dagger \mathbf{M}^{-1} \mathbf{s}|^2}{\mathbf{s}^\dagger \mathbf{M}^{-1} \mathbf{s}}} \right)} u(\mathbf{z}^\dagger \mathbf{M}^{-1/2} \Sigma \mathbf{M}^{-1/2} \mathbf{z}) \underset{H_0}{\overset{H_1}{\geq}} G \quad (21)$$

Denote by l_{NMF} the normalized matched filter (NMF),

$$l_{\text{NMF}} = \frac{|\mathbf{z}^\dagger \mathbf{M}^{-1} \mathbf{s}|^2}{(\mathbf{z}^\dagger \mathbf{M}^{-1} \mathbf{z})(\mathbf{s}^\dagger \mathbf{M}^{-1} \mathbf{s})} \quad (22)$$

Finally, the GLRT-based test (21) can be recast as

$$\frac{1}{(\sqrt{1 - l_{\text{NMF}}} \gamma \sqrt{l_{\text{NMF}}})^2} u \left(\mathbf{z}^\dagger \mathbf{M}^{-1/2} \boldsymbol{\Sigma} \mathbf{M}^{-1/2} \mathbf{z} \right) \underset{H_0}{\overset{H_1}{\geq}} G \quad (23)$$

Expression (23) highlights that the GLRT only depends on NMF and γ , linking to mismatched angle ϕ .

3. ADAPTIVE SCHEMES

In practical applications, the power spectral density of clutter is usually unknown, a suitable estimation is required in place of the exact covariance structure \mathbf{M} to devise a fully adaptive detector. Assume the secondary data $\mathbf{X} = [\mathbf{x}_1, \mathbf{x}_2 \dots, \mathbf{x}_K] \in \mathbb{C}^{N \times K}$ with size K , which are independent identically distributed vectors with free of the signal components, sharing the same covariance structure with the primary data, are available.

There are three common estimation strategies, i.e., sample covariance matrix (SCM), normalized sampled covariance matrix (NSCM), and fixed point estimation (FPE) matrix. In general, the SCM performs well in Gaussian interference, and guarantees the CFAR property with respect to the covariance matrix. However, in non-Gaussian clutter, it is no longer ensuring CFAR property with respect to the power levels. For NSCM, it is biased and not consistent [16], and is not CFAR with respect to the covariance matrix in SIRVs. As to FPE, it performs well in SIRVs, and is unbiased, consistent and ensures the CFAR property with respect to both the structure of the covariance matrix and the clutter power levels.

Thus, we focus on the FPE method, which is given by

$$\widehat{\mathbf{M}}_{\text{FEP}} = \frac{N}{K} \sum_{k=1}^K \frac{\mathbf{x}_k \mathbf{x}_k^\dagger}{\mathbf{x}_k^\dagger \widehat{\mathbf{M}}_{\text{FEP}}^{-1} \mathbf{x}_k} \quad (24)$$

To solve the FPE of (24), it can be resorted to the recursive operation, i.e.,

$$\widehat{\mathbf{M}}_{\text{FEP}}(\ell + 1) = \frac{N}{K} \sum_{k=1}^K \frac{\mathbf{x}_k \mathbf{x}_k^\dagger}{\mathbf{x}_k^\dagger \widehat{\mathbf{M}}_{\text{FEP}}^{-1}(\ell) \mathbf{x}_k}, \quad \ell = 0, 1, \dots, L_{\text{FEP}} \quad (25)$$

and the initial estimate $\widehat{\mathbf{M}}_{\text{FEP}}(0)$ is given by

$$\widehat{\mathbf{M}}_{\text{FEP}}(0) = \frac{N}{K} \sum_{k=1}^K \frac{\mathbf{x}_k \mathbf{x}_k^\dagger}{\mathbf{x}_k^\dagger \mathbf{x}_k} \quad (26)$$

The recursive error is defined as

$$\text{ER}(\ell) = \frac{\left\| \widehat{\mathbf{M}}_{\text{FEP}}(\ell+1) - \widehat{\mathbf{M}}_{\text{FEP}}(\ell) \right\|_F}{\left\| \widehat{\mathbf{M}}_{\text{FEP}}(\ell+1) \right\|_F} \quad (27)$$

where $\|\cdot\|_F$ denotes the Frobenius norm and L_{FEP} denotes the number of the recursion. In general, the L_{FEP} is less than 5 for $\text{ER} < 5\%$. Therefore, the FPE is also called recursive ML-estimator.

Hence, the two-step adaptive GLRT-based test is given by

$$\frac{1}{\left(\sqrt{1 - \hat{l}_{\text{NMF}}} - \gamma \sqrt{\hat{l}_{\text{NMF}}} \right)} u \left(\mathbf{z}^\dagger \widehat{\mathbf{M}}^{-1/2} \widehat{\boldsymbol{\Sigma}} \widehat{\mathbf{M}}^{-1/2} \mathbf{z} \right) \underset{H_0}{\overset{H_1}{\gtrless}} G_1 \quad (28)$$

where

$$\hat{l}_{\text{NMF}} = \frac{\left| \mathbf{z}^\dagger \widehat{\mathbf{M}}_{\text{FEP}}^{-1} \mathbf{s} \right|^2}{\left(\mathbf{z}^\dagger \widehat{\mathbf{M}}_{\text{FEP}}^{-1} \mathbf{z} \right) \left(\mathbf{s}^\dagger \widehat{\mathbf{M}}_{\text{FEP}}^{-1} \mathbf{s} \right)} \quad (29)$$

and G_1 is the suitable modification of the original threshold in (23).

4. PERFORMANCE ASSESSMENT

This section is devoted to the evaluation of the proposed receiver in terms of the probabilities of detection (P_d) and false alarm (P_{fa}). Consider a uniform linear array with N omni-directional elements, and the nominal steering vector \mathbf{s} is given by

$$\mathbf{s} = \frac{1}{\sqrt{N}} [1, 1, \dots, 1]^T \quad (30)$$

The actual received steering vector after whitening and rotating is given

$$\mathbf{p} = A \exp \{j\xi\} \left(\mathbf{e}_N \cos \phi + \frac{\mathbf{e}_N^\perp}{\|\mathbf{e}_N^\perp\|} \sin \phi \right) \quad (31)$$

where A is the amplitude, ξ is the random phase, \mathbf{e}_N^\perp is a complex vector, orthogonal to \mathbf{e}_N , with independent identically distributed

complex Gaussian random components, and ϕ is the mismatches acute angle between actual steering vector and nominal vector, such that

$$\cos \phi = \frac{|\mathbf{p}^\dagger \mathbf{e}_N|}{\|\mathbf{p}\| \|\mathbf{e}_N\|} \tag{32}$$

We assume a clutter-dominated scenario, which is sampled from K -distribution random vector with exponential correction shape of covariance structure, such that

$$\mathbf{M}(k, j) = \rho^{|k-j|}, \quad 1 \leq k, \quad j \leq N \tag{33}$$

where ρ is the one-lag correlation coefficient. The signal-to-clutter ratio (SCR) is defined as

$$\text{SCR} = A^2 \mathbf{s}^\dagger \mathbf{M}^{-1} \mathbf{s} \tag{34}$$

Since closed-form expressions of detection probability (P_d) and false alarm probability (P_{fa}) are not available, we resort to standard Monte Carlo technologies. To limit the computation burden, we assume $P_{fa} = 10^{-3}$.

In Figure 2, we analyze the impact of the mismatched angle ϕ on the detection performance, where P_d s of adaptive GLRT and NMF are plotted versus SCR for $P_{fa} = 10^{-3}$, $N = 8$, $K = 32$, $\nu = 0.5$, $\gamma = 0.5$, $\rho = 0.9$, and several values of $\cos \phi$. The curves show

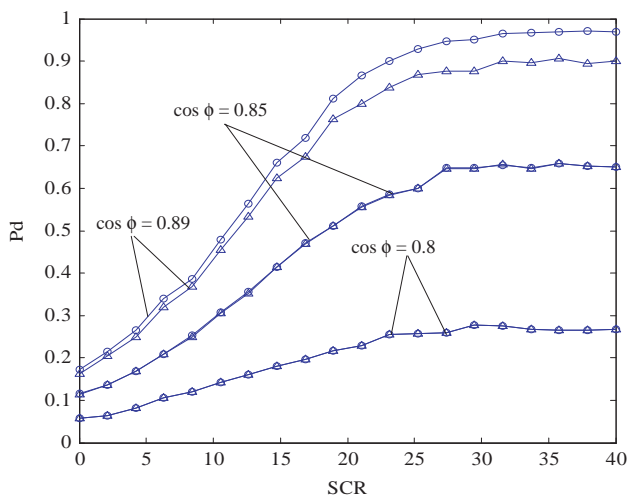


Figure 2. P_d plots v.s. SCR with $\cos \phi = 0.89, 0.85, 0.8$, “o” curves NMF, “ Δ ” curves GLRT, for $P_{fa} = 10^{-3}$, $N = 8$, $K = 32$, $\nu = 0.5$, $\gamma = 0.5$, $\rho = 0.9$, and non-fluctuating target.

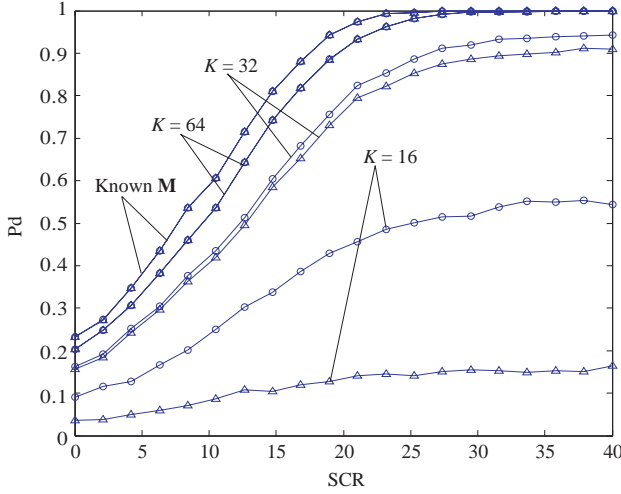


Figure 3. P_d plots v.s. SCR with $K = 16, 32, 64$, “o” curves NMF, “ Δ ” curves GLRT, for $P_{fa} = 10^{-3}$, $N = 8$, $\nu = 0.5$, $\gamma = 0.5$, $\cos \phi = 0.89$, $\rho = 0.9$, and non-fluctuating target.

that the detection performance is decreased when decreasing $\cos \phi$, in other words, for large ϕ , the mismatches loss are more serious. At such case, the adaptive GLRT is prone to reject the signals, although the SCR is high. Moreover, the adaptive GLRT is consistent with adaptive NMF in large mismatched angle. In high $\cos \phi$, the detection performance of the NMF is a little better, or the GLRT has better rejection performance for mismatched signals.

The influence of the size K of the secondary data is analyzed in Figure 3, where P_d s of adaptive GLRT and NMF are plotted versus SCR for several values of K , together with exact covariance structure. It is evident that detection performance is increased when increasing the size K , and the adaptive loss is acceptable. Specifically, the loss is 2 dB in the case $P_d = 0.9$ between exact covariance and estimated covariance with $K = 64$. Meanwhile, the derived adaptive GLRT is consistent with adaptive NMF in large size case, however, in the small size K , the detection performance of NMF is better.

In the sequel we assess the performance of the proposed GLRT in the presence of fluctuating targets. To this end, we assume that the amplitude A is distributed as a chi random variable with $2m$ degrees of freedom [5],

$$f_A(x) = 2 \left(\frac{m}{A^2} \right)^m \frac{x^{2m-1}}{\Gamma(m)} \exp\left(-\frac{m}{A^2}x^2\right) u(x), \quad m > 0 \quad (35)$$

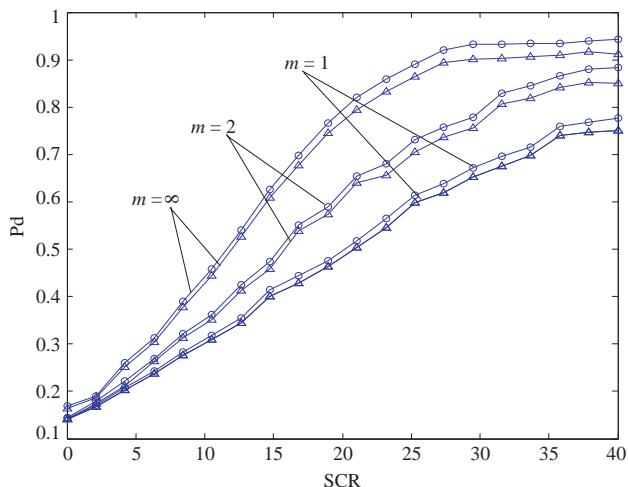


Figure 4. P_d plots v.s. SCR with different fluctuating model, “o” curves NMF, “ Δ ” curves GLRT, for $P_{fa} = 10^{-3}$, $N = 8$, $\nu = 0.5$, $K = 32$, $\gamma = 0.5$, $\cos \phi = 0.85$, $\rho = 0.9$ and fluctuating target.

The parameter m rules the depth of the amplitude fluctuation: the lower the shape parameter m , the wider the fluctuation span. Notice that model (35) subsumes, as special cases, both the Rayleigh distribution and non-fluctuating amplitude, for $m = 1$ or $m = +\infty$, respectively. In Figure 4, the P_d s of adaptive GLRT and NMF are plotted versus average SCR, i.e.,

$$SCR = \bar{A}^2 \mathbf{s}^\dagger \mathbf{M}^{-1} \mathbf{s} \tag{36}$$

The results show that the fluctuation law significantly affects the detection performance, the larger the m , the better the detection performance. It is because for the larger value of m , the fluctuation is more prone to non-fluctuation characteristics.

5. CONCLUSIONS

In this paper, we address the receiver design against SIRV clutter in the presence of steering vector mismatches with unknown power spectral density, and the fully adaptive GLRT-based receiver is devised resorting to the secondary data.

Several numerical simulations are provided, and the results highlight that the derived GLRT is in accordance with adaptive NMF in exact covariance case or/and serious mismatched cases. Meanwhile,

the detection performance also depends on the fluctuating depth of the target, the deeper the fluctuations, the worse the detection performance.

Possible future research tracks might concern the assessment of the mismatched case for polarimetric [18] and colocated MIMO radars [19] in SIRV clutter.

ACKNOWLEDGMENT

This work is sponsored by Sichuan Youth Science and Technology Foundation (2011JQ0024) and the Fundamental Research Funds for the Central Universities (103.1.2-E022050205).

REFERENCES

1. Kelly, E. J., "An adaptive detection algorithm," *IEEE Trans. on Aerospace and Electronic Systems*, Vol. 22, No. 1, 115–127, Mar. 1986.
2. Robey, F. C., D. R. Fuhrmann, R. Nitzberg, and E. J. Kelly, "A CFAR adaptive matched filter detector," *IEEE Trans. on Aerospace and Electronic Systems*, Vol. 28, No. 1, 208–216, Jan. 1992.
3. Conte, E., M. Lops, and G. Ricci, "Adaptive matched filter detection in spherically invariant noise," *IEEE Signal Processing Letter*, Vol. 3, No. 8, 248–250, Aug. 1996.
4. Kraut, S., L. L. Scharf, and L. T. McWhorter, "Adaptive subspace detectors," *IEEE Trans. on Signal Processing*, Vol. 49, No. 1, 1–16, Jan. 2001.
5. De Maio, A., "Robust adaptive radar detection in the presence of steering vector mismatches," *IEEE Trans. on Aerospace and Electronic Systems*, Vol. 41, No. 4, 1322–1337, Oct. 2005.
6. Bandiers, F., A. De Maio, and G. Ricci, "Adaptive CFAR radar detection with conic rejection," *IEEE Trans. on Signal Processing*, Vol. 55, No. 6, 2533–2541, Jun. 2007.
7. Bandiers, F., D. Orlando, and G. Ricci, "CFAR detection strategies for distributed targets under conic constraints," *IEEE Trans. on Signal Processing*, Vol. 57, No. 9, 3305–3316, Sep. 2009.
8. Besson, O., "Adaptive detection with bounded steering vector mismatch angle," *IEEE Trans. on Signal Processing*, Vol. 55, No. 4, 1560–1564, Apr. 2007.

9. Conte, E. and M. Longo, "Modelling and simulation of non-Rayleigh radar clutter," *IEE Proceedings F*, Vol. 138, No. 2, 121–130, 1991
10. Sangston, K. and K. Gerlach, "Coherent detection of radar targets in a non-Gaussian background," *IEEE Trans. on Aerospace and Electronic Systems*, Vol. 30, No. 2, 330–340, 1994.
11. Conte, E., M. Lops, and G. Ricci, "Asymptotically optimum radar detection in compound-Gaussian clutter," *IEEE Trans. on Aerospace and Electronic Systems*, Vol. 31, No. 2, 611–616, Apr. 1995.
12. Tatarskii, V. I. and V. V. Tatarskii, "Statistical non-Gaussian model of sea surface with anisotropic spectrum for wave scattering theory. Part I," *Progress In Electromagnetics Research*, Vol. 22, 259–291, 1999.
13. Tatarskii, V. I. and V. V. Tatarskii, "Statistical non-Gaussian model of sea surface with anisotropic spectrum for wave scattering theory. Part II," *Progress In Electromagnetics Research*, Vol. 22, 293–313, 1999.
14. Younsi, A. and M. Nadour, "Performance of the adaptive normalized matched filter detector in compound-Gaussian clutter with inverse Gamma texture model," *Progress In Electromagnetics Research B*, Vol. 32, 21–38, 2011.
15. Gini, F. and M. V. Greco, "Covariance matrix estimation for CFAR detection in correlated heavy tailed clutter," *Signal Processing*, Vol. 82, No. 12, 1847–1859, Dec. 2002.
16. Pascal, F., Y. Chitour, J. P. Ovarlez, P. Forster, and P. Larzabal, "Covariance structure maximum-likelihood estimates in compound Gaussian noise: Existence and algorithm analysis," *IEEE Trans. on Signal Processing*, Vol. 56, No. 1, 34–48, Jan. 2008.
17. Pascal, F., P. Forster, J. P. Ovarlez, and P. Larzabal, "Performance analysis of covariance matrix estimates in impulsive noise," *IEEE Trans. Signal Processing*, Vol. 56, No. 6, 2206–2217, Jun. 2008.
18. De Maio, A., G. Alfano, and E. Conte, "Polarization diversity detection in compound-Gaussian clutter," *IEEE Trans. on Aerospace and Electronic Systems*, Vol. 10, No. 1, 114–131, Aug. 2004.
19. Li, J. and P. Stoica, "MIMO radar with colocated antennas," *IEEE Signal Processing Magazine*, Vol. 24, No. 5, 106–114, Oct. 2007.